Applied Energy 172 (2016) 398–407

Contents lists available at ScienceDirect

Applied Energy

journal homepage: www.elsevier.com/locate/apenergy

Development of an empirical aging model for Li-ion batteries and application to assess the impact of Vehicle-to-Grid strategies on battery lifetime

Martin Petit *, Eric Prada, Valérie Sauvant-Moynot

IFP Energies nouvelles, Rond-point de l'échangeur de Solaize, BP3, 69360 Solaize, France

HIGHLIGHTS

- Empirical capacity loss model for Li-ion batteries.
- Both calendar and cycle aging were modeled.
- Calibrated and validated on LFP/C and NCA/C cells using experimental data.
- Real life application to assess the influence of V2G on aging for both technologies.

GRAPHICAL ABSTRACT

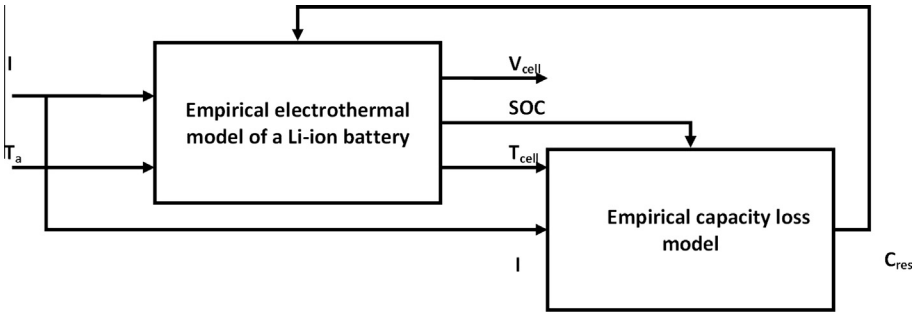

ARTICLE INFO

Article history:
Received 21 January 2016
Received in revised form 10 March 2016
Accepted 30 March 2016
Available online 22 April 2016

Keywords:
Lithium-ion
Aging modeling
Vehicle-to-grid
Electric vehicle

ABSTRACT

In this paper an empirical capacity fade model for Li-ion batteries has been developed, calibrated and validated for a NCA/C and a LFP/C Li-ion cell. Based on extensive experimental work, this original, generic model is well suited for system simulation approaches, and is able to describe both cycle and calendar effects on aging. The stress factors taken into account for each aging mode are the state of charge and the temperature for calendar aging, and the temperature and the current for cycle aging. A simple approach has been adopted in order to instantaneously apply either cycle aging or calendar aging according to operating conditions and thus accurately model aging effects due to dynamic operating conditions. This model has then been coupled to an electrothermal model and integrated in a system simulation software application in order to assess the effect of charging rates, charging strategies and V2G on battery lifetime. When compared, the two battery chemistries exhibited different behaviors when submitted to V2G scenarios. Light V2G scenarios caused relatively low aging for the LFP/C based battery but tended to slightly increase the aging of the NCA/C based battery according to simulations.

© 2016 Elsevier Ltd. All rights reserved.

1. Introduction

In order to reduce fossil energy dependence and the environmental impact of vehicles, new regulations are encouraging car manufacturers toward vehicle electrification. This trend raises the issue of electrical energy storage. Li-ion batteries are one of the most promising solutions to store the energy needed for highly electrified vehicles: hybrid electrical vehicles (HEV), plug-in hybrid vehicles (PHEV) or full electric vehicles (EV). However, energetic and power performance of Li-ion batteries is known to decrease during their service lifetime [1].

Although the cost of battery packs is decreasing [2], they comprise a significant proportion of market vehicle price, which means car manufacturers have to provide a guaranteed longevity ensuring

* Corresponding author.
E-mail address: martin.petit@ifpen.fr (M. Petit).

http://dx.doi.org/10.1016/j.apenergy.2016.03.119
0306-2619/© 2016 Elsevier Ltd. All rights reserved.

a safe and sufficient battery performance throughout the vehicle service lifetime. Therefore, battery aging studies are of particular interest in order to optimize battery systems in terms of size and cooling requirements, and also to devise management strategies well suited along the vehicle lifetime. Providing a minimum level of performance is also mandatory to ensure financial viability for electrified vehicles. For such concerns, modeling is essential to provide car designers with information and reduce development costs.

While the main microscopic aging phenomena of Li-ion cells have been identified [1,3] and described, for instance Li plating at low temperature [4], loss of active material at elevated temperature [5] or solid electrolyte interphase (SEI) growth at the negative electrode/electrolyte interface [6,7], aging of Li-ion batteries remains difficult to predict [8,9]. In most aging models, considering that SEI growth is the main cause of aging for Li-ion batteries with graphite negative electrode leads to a quadratic evolution shape of the capacity loss in the beginning of the battery life as put forward by Spotnitz [10].

To find the main impact factors, research efforts have been dedicated to model macroscopic Li-ion cell capacity loss and impedance increase [11,12]. The main aging factors are the state of charge, *SOC*, the depth of discharge during cycle, *DoD*, the temperature, *T*, and current, *I*. Another key impact factor is the battery usage [13] which can be described in two contributions to aging:

- Calendar aging ($I = 0$): the battery is stored without being used so there is no current through the battery.
- Cycle aging ($I \neq 0$): the battery is either charged or discharged.

It has been shown that the two types of aging will lead to different battery behaviors with usually a higher capacity loss and higher power loss during cycle aging [13].

In order to model aging phenomena, two different approaches have been put forward in the literature, which are physical modeling [14–16] and empirical modeling [10,17]. Usually empirical models will address either calendar aging [10,13] or cycle aging [11]. Some other modeling works include both cycle and calendar aging behaviors [18–20] but, despite describing cycle aging, the proposed model did not take into account the charging rate on aging. The resulting model assesses the capacity loss as a function of time and constant stress factors which has little application in use [21–24]. It is not convenient to use this kind of modeling for system simulation where stress factors are dynamically varying, for instance due to environmental conditions (temperature variations due to seasons and day and night successions) or due to vehicle use (storage SOC depending on the duty cycle).

In this paper, we introduce an original empirical capacity fade model suitable for system simulation application. This generic approach for Li-ion batteries is applied on two Li-ion technologies and validated against experimental data. Once validated, it can be used in a system simulation to assess the usefulness of different charging strategies in order to preserve the batteries' performance throughout their lifetime in various realistic operating conditions.

2. Model development

The capacity fade model is based on 2 contributions leading to different capacity losses in Ah: Q_{loss}^{cal} due to calendar aging and Q_{loss}^{cyc} due to cycle aging.

2.1. Calendar aging

As often discussed the two main stress factors for calendar aging are temperature and State of Charge (SOC). Usually [11,22,25] an empirical aging law is given as below

$$Q_{loss}^{cal} = B_{cal}(SOC)\exp\left(-\frac{Ea_{cal}}{RT}\right)t^{z_{cal}} \quad (1)$$

In this expression B_{cal} is a pre-exponential factor depending on *SOC*, expressed in $\frac{Ah}{s^{z_{cal}}}$, Ea_{cal} is the activation energy, expressed in J mol^{-1}, which evaluates the dependency of calendar aging on temperature *T*, expressed in K, and z_{cal} is a dimensionless constant. Considering a capacity loss phenomenon linked to SEI growth and diffusion limitations, this exponent should be around 0.5.

This expression is well suited to rapidly evaluate the capacity lost during long term storage but it is not suitable when many different operating conditions are happening. As a consequence, this expression has been differentiated against time in order to evaluate infinitesimal variation of capacity due to calendar aging:

$$\frac{dQ_{loss}^{cal}}{dt} = z_{cal}B_{cal}(SOC)\exp\left(-\frac{Ea_{cal}}{RT}\right)\left(\frac{Q_{loss}^{cal}}{B_{cal}(SOC)\exp\left(-\frac{Ea_{cal}}{RT}\right)}\right)^{1-\frac{1}{z_{cal}}} \quad (2)$$

This expression can then be linked to other capacity loss phenomena like cycle aging.

2.2. Cycle aging

For cycle aging a similar approach based on Wang et al. [11] is used. In this study the capacity loss due to aging is influenced by two major stress factors: current and temperature. The formulation encountered is then:

$$Q_{loss}^{cyc} = B_{cyc}\exp\left(\frac{-Ea_{cyc}+\alpha|I|}{RT}\right)Ah^{z_{cyc}} \quad (3)$$

In this expression, B_{cyc} is a pre exponential factor in $Ah^{1-z_{cyc}}$ which depends on current, Ea_{cyc} is an activation energy for cycle aging expressed in J mol^{-1}, α is a coefficient for aging acceleration due to current expressed in J mol^{-1} A^{-1}, z_{cyc} is an exponent constant that should be around 0.5 for diffusion limited process. Finally, *Ah* stands for Ah throughput, that is the amount of charge sent into the cell. For the same reason as for calendar aging, this expression has been differentiated against time:

$$\frac{dQ_{loss}^{cyc}}{dt} = \frac{|I|}{3600}z_{cyc}B_{cyc}(I)\exp\left(\frac{-Ea_{cyc}+\alpha|I|}{RT}\right)\left(\frac{Q_{loss}^{cyc}}{B_{cyc}(I)\exp\left(\frac{-Ea_{cyc}+\alpha|I|}{RT}\right)}\right)^{1-\frac{1}{z_{cyc}}} \quad (4)$$

In this expression, the Ah throughput term, once differentiated, is proportional to the current in the cell.

2.3. Switch between calendar and cycle aging

Once the influence on aging has been expressed for both behaviors, it is necessary to find a way to decide what kind of aging is occurring based on the actual operating conditions. In some approaches it has been assumed that the cycle aging contribution does not take into account calendar effects [22,23]. Both contributions are then added to get the total aging. In our work, the assumption is that when the modeling of cycle aging has been performed, calendar aging occurring during cycle mode is already taken into account. As a consequence, we need to find a condition describing the switch between calendar and cycle mode.

First, taking as a major phenomenon of capacity loss the SEI formation at the negative electrode, it is known that the parasitic reaction of SEI formation is accelerated when the negative electrode potential is lower (i.e. during charge or when the SOC is high). As a consequence it has been assumed that cycle aging only occurs when the battery is in charge and the current is above a

given threshold I_{cyc} since higher charging current will lead to lower potential at the negative electrode. Furthermore, in order to assess the fact that diffusion in the cell tends to increase the overpotential when the charge is longer and then increases the rate of the SEI formation reaction, the current in $\frac{dQ_{loss}^{cyc}}{dt}$ expression (4) is replaced by a filtered current $\bar{I}$. As a consequence the total capacity loss is computed as follows:

$$\frac{dQ_{loss}}{dt} = \begin{cases} \frac{dQ_{loss}^{cal}}{dt} & \Longleftrightarrow \bar{I} < I_{cyc} \\ \frac{dQ_{loss}^{cyc}}{dt} & \Longleftrightarrow \bar{I} > I_{cyc} \end{cases} \quad (5)$$

This given threshold will depend on the battery's ability to tackle high charging rates. For example high power batteries should have a high threshold around $1I_t$ (the current in A needed to deplete the battery in 1 h) whereas high energy batteries designed for lower charging rates should have a lower threshold.

2.4. Coupling with an electrothermal model of the battery behavior

In order to get a global model of the electrothermal behavior of a Li-ion cell, it is necessary to couple this aging model with an electrothermal model. In this study a quasistatic electrical circuit equivalent model was chosen, similar to the one present in LMS Imagine.Lab Amesim™ Electrical Storage Library [26]; although other types of modeling approach like dynamic electrical circuit equivalent [27] or even electrochemical approach [28] can be used. In Fig. 1 are represented the inputs and outputs of both models as well as the coupling involved.

The electrothermal model evaluates the state of charge (SOC), the voltage (V_{cell}) and the temperature (T_{cell}) of the battery based on the input current (I) and external temperature (T_a). It provides the empirical aging model with the SOC and the T_{cell} allowing it to evaluate the residual capacity C_{res}. This residual capacity is then used in the electrothermal model to evaluate the SOC as follows:

$$SOC = SOC_0 + \frac{100}{3600}\int_0^t \frac{I}{C_{res}(t)}dt \quad (6)$$

3. Experimental validation

3.1. Calibration data

In order to calibrate the empirical model presented in this paper, extensive experimental data are needed spanning a wide range of operating conditions representative of the battery use. Experimental campaigns have been carried out by research groups in order to assess both cycle and calendar behavior of Li-ion batteries [12,18,20,25,29,30]. Two sets of calibration data are indeed necessary in order to take into account both types of aging. In these sets, experiments highlighting every stress factor are needed. As a consequence a significant amount of experimental data was collected in the literature for calendar aging [31] as well as for cycle aging [11,32].

Thanks to these data, it has been possible to calibrate the capacity loss model on two different battery technologies:

- A123s 2.3 Ah LFP/C cell.
- Saft VL6P 7 Ah NCA/C cell.

The parameters used for these technologies are indicated in Table 1. In the following section we will discuss in detail the validation for the A123s model.

3.2. Validation of empirical model

3.2.1. Synthetic profiles

Extensive experimental studies from Savoye [33] have subjected several A123s 2.3 Ah cells to various cycle conditions in order to evaluate the cycling impact on Li-ion battery aging. The aim was to discuss the aging impact in an automotive application and especially the impact of short current pulses on aging. The current profiles represented in Fig. 2 are looped at 25 °C and 45 °C over more than 4000 cycles. These current profiles interestingly cover various cycle profiles with highly dynamic pulses at several different rates (ISO RMS and ISO MEAN), moderately dynamic pulses (DILATED) and slow solicitations (REFERENCE or 0.8 REFERENCE), as well as mixed solicitations (AT REST).

The comparison between experimental and simulation results using the empirical aging model described above is presented in Fig. 3. Note that two cells were tested for each condition. This figure shows a good agreement between experimental results and simulations with less than 5% error for capacity loss lower than 20%, except for the ISO MEAN condition where the model overestimates the capacity loss by 14%. These results seem encouraging for using this model in automotive applications.

3.2.2. Road profile

In order to further validate the empirical model on actual data representative of vehicle use, aging measurements have been performed at cell level on IFPEN test benches [34]. Realistic EV and HEV system simulations were carried out [35] in order to obtain two different road profiles, which were then looped. For the EV load profile (Fig. 4a), the program consisted of four charge depleting cycles followed by a constant current charge in order to get back to the initial SOC. The HEV load profile (Fig. 4b) consists of a charge-sustaining current profile which maintains the SOC around 60%. The maximum current involved in the HEV profile is around 50 A whereas it remains lower than 20 A in the EV profile.

In Fig. 5, it is possible to verify that the model is able to predict accurately capacity loss for both aging patterns (EV in Fig. 5a and HEV in Fig. 5b). It is then possible to use this model in an automotive application.

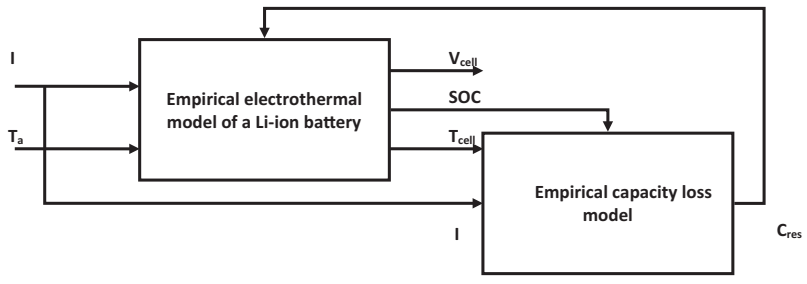

Fig. 1. Representation of the coupling between an electrothermal model and the empirical aging model.

Table 1
Parameters of the empirical aging model.

	A123s 2.3 Ah				Saft VL6P		
Calendar aging							
$B_{cal}(SOC)$	30%	65%	100%		30%	65%	100%
	$7.34 \cdot 10^5$	$6.75 \cdot 10^5$	$2.18 \cdot 10^5$		$2.78 \cdot 10^5$	$3.80 \cdot 10^5$	$5.43 \cdot 10^5$
$Ea_{cal}(SOC)$	30%	65%	100%			52,862 J/mol	
	73,369 J/mol	69,804 J/mol	56,937 J/mol				
$z_{cal}(SOC)$	30%	65%	100%			0.52	
	0.943	0.900	0.683				
Cycling aging							
$B_{cyc}(I)$	1 A	4 A	12 A	20 A		130	
	$3.16 \cdot 10^3$	$2.17 \cdot 10^4$	$1.29 \cdot 10^4$	$1.55 \cdot 10^4$			
Ea_{cyc}	31,700 J/mol					18,461 J/mol	
z_{cyc}	0.55					0.4	
α_{cyc}	370.3					32	
I_{cyc}	1 I_t					1 I_t	
τ_{filt}	60 s					0 s	

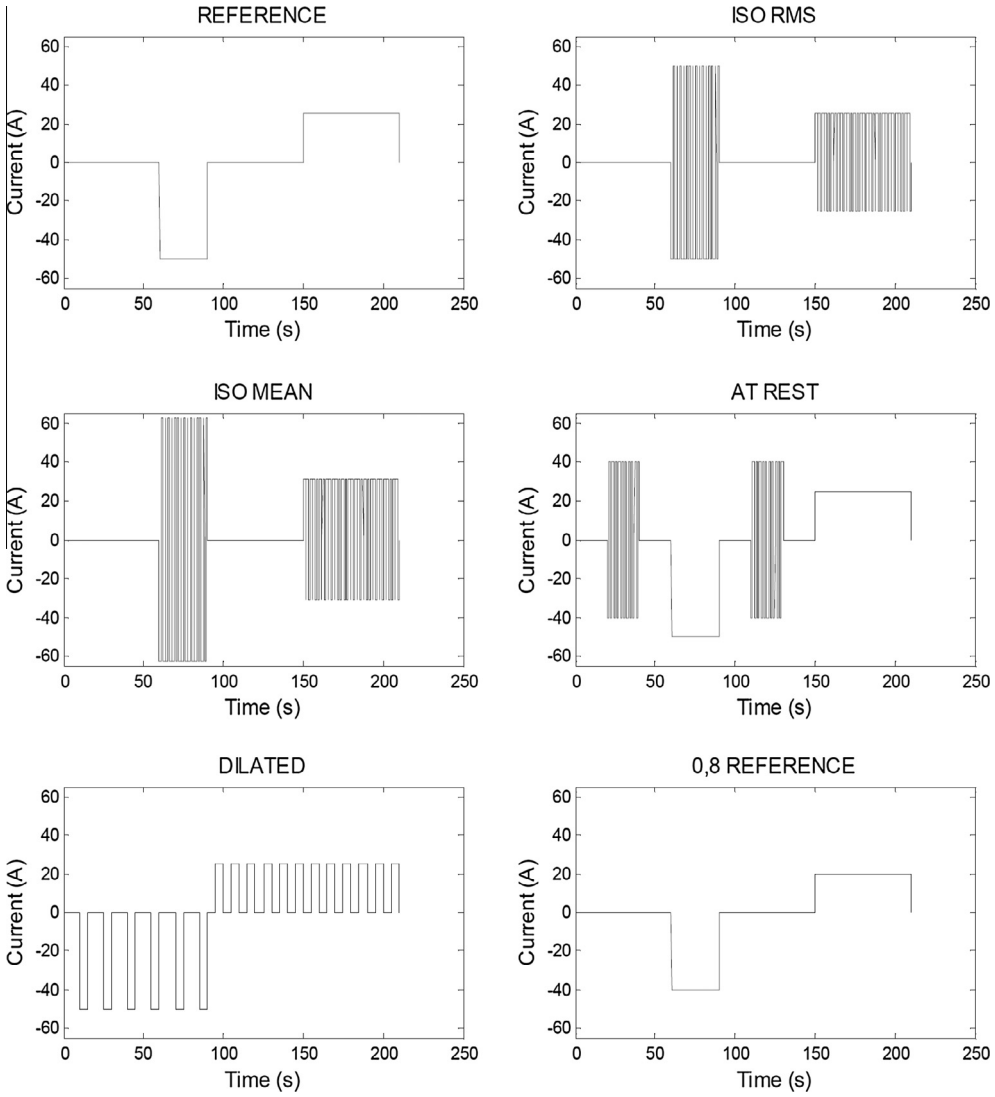

Fig. 2. Current profile taken from Savoye [33].

4. Applications for lifetime prediction

This capacity loss empirical model has been implemented in LMS Imagine.Lab Amesim™ dedicated to system simulation. It can then be used in realistic operating conditions in order to adapt the charging strategies taking into consideration the long term issue of aging. In this scope we focused on a study that will discuss the impact of the recharge strategy of an

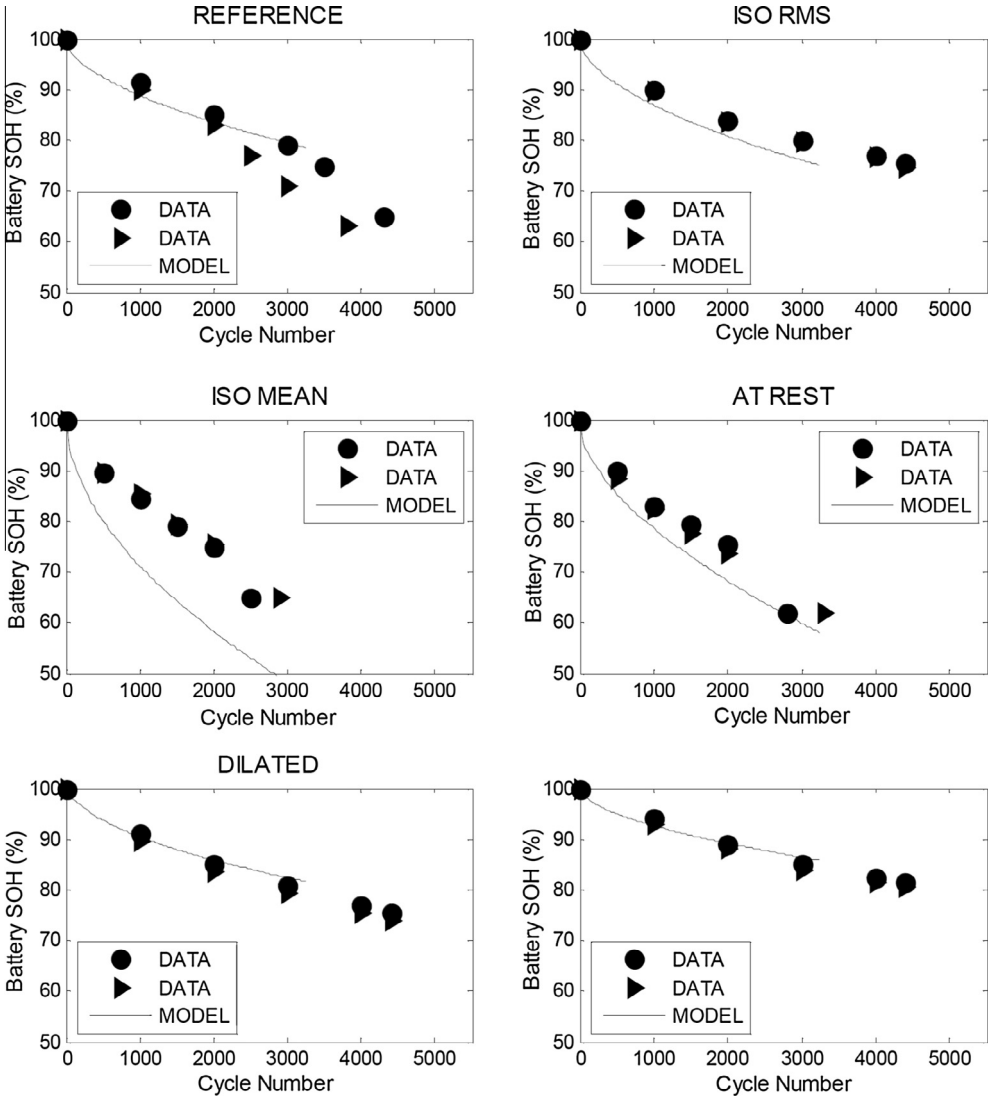

Fig. 3. Comparison between experimental data from Savoye [33] and simulation results.

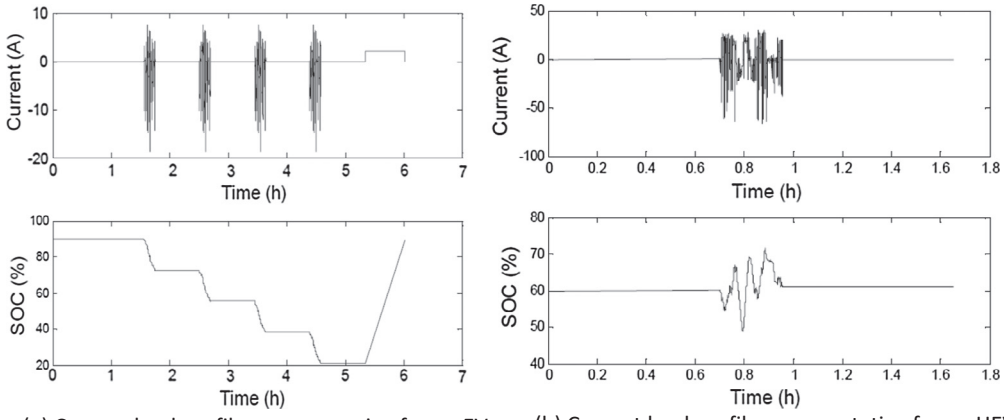

(a) Current load profile representative for an EV and subsequent SOC profile

(b) Current load profile representative for an HEV and subsequent SOC profile

Fig. 4. Current profile used for EV and HEV validation.

electric vehicle fitted with a LFP–C battery or a NCA–C battery.

One of the key stress factors of aging is the temperature conditions to which the car is submitted. Fig. 6 illustrates the temperature variations seen by the battery during a year in our case studies. There is in fact a double temperature variation. External temperature is submitted to a daily variation due to days and nights but also to an annual variation due to seasons. Moreover,

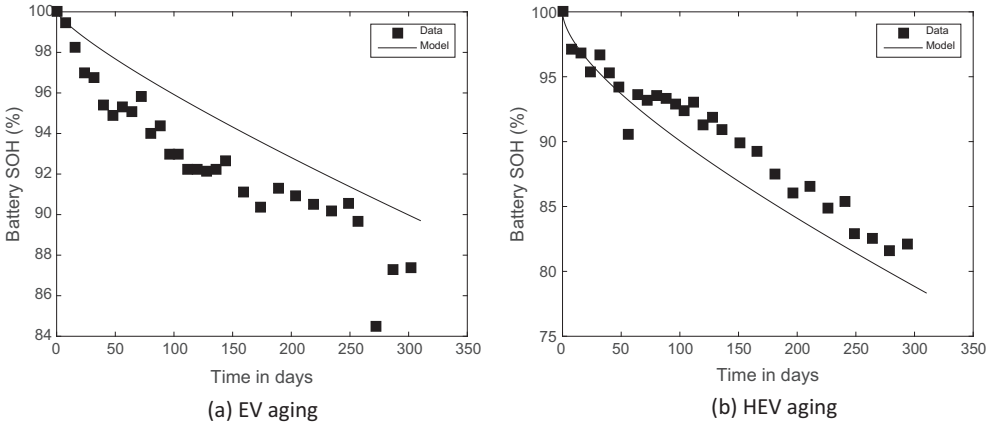

Fig. 5. Comparison between experimental data and simulation results.

the use of the battery leads to a temperature increase due to heat losses. As can be seen in the prediction of battery daily temperature variations some small peaks mark a battery self-heating of 1 or 2 °C under the hypothesis of an efficient thermal exchange leading to an exchange coefficient of 50 W/m^2/K.

As far as the daily duty cycle of the vehicle is concerned, it can be simplified with a common pattern comprising charging phases and trips from home to work and back as proposed by Guenther et al. [22]. The base case which is considered in this study is the following:

– 4 home-work trips lasting 20 min at 8 AM, 12 PM, 1 PM and 6 PM.

In order to get realistic and fit-for-purpose road profile patterns, the electric vehicle simulator developed by Badin et al. [35] has been used to synthesize the power demands on the electrical storage system when the vehicle is submitted to an NEDC cycle. This NEDC power demand is then used for each home-work trip.

Two different factors are studied here, with first the influence of the charging rate on the battery lifetime expectancy and then the influence of Vehicle-to-Grid (V2G) on the battery aging during one calendar year. Simulations have been performed on both LFP/C and NCA/C packs whose properties are given in Table 2. The aim was to build a battery pack with the same capacity. The NCA/C cell properties have been scaled in order to match the A123s nominal capacity. Its nominal capacity has been set to 2.3 Ah and its internal resistance has been multiplied by a scaling coefficient. However due to the differences between the nominal voltage and inherent properties of the cells such as internal resistance, the pack power and energy are different.

Table 2
Battery pack properties for simulations.

Chemistry of battery cells	LFP/C	NCA/C
Capacity of the battery	2.3 Ah	2.3 Ah
Number of cells in series	100	100
Number of parallel branches	10	10
Power of the pack	384 kW	189 kW
Energy of the pack	7600 Wh	8280 Wh
Nominal voltage of the pack	320 V	360 V

4.1. Influence of charging rate

In order to study the influence of charging rate, the LFP/C battery pack is charged at the end of the day (starting at 7 PM) at various charging rates (1/6 I_t, 1/3 I_t, 1/2 I_t, I_t, 2 I_t, 3I_t and 4 I_t). The daily current profile can be seen in Fig. 7a. The only visible variation between the simulations is the charge where the input current varies from 3.83 A to 96 A and the charging time accordingly from 3.5 h to 10 min.

As can be seen in Fig. 7b, the lifetime expectancy, being the time before the capacity loss of the battery reaches 20% of the initial nominal capacity, decreases as the charging rate increases from 7.3 years to 5.57 years. It is worth noting that the lifetime for charging rates higher than I_t are in a close range between 5.57 and 5.74 years. This result is due to two factors: the higher charging current accelerates the battery degradation increasing the capacity loss due to cycling aging. This effect can be seen in simulation where charging rate is below 1 I_t. Then, due to the fast charge, the battery stays at higher SOC for a longer time increasing the capacity loss due to calendar aging. For higher charging rates,

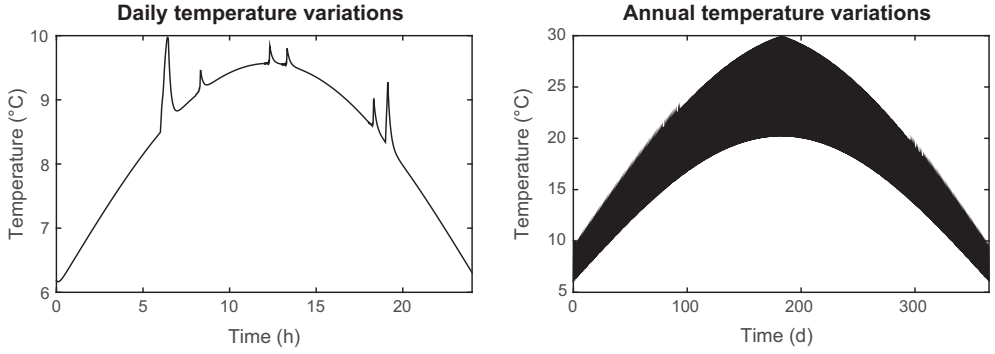

Fig. 6. Temperature variations during simulation.

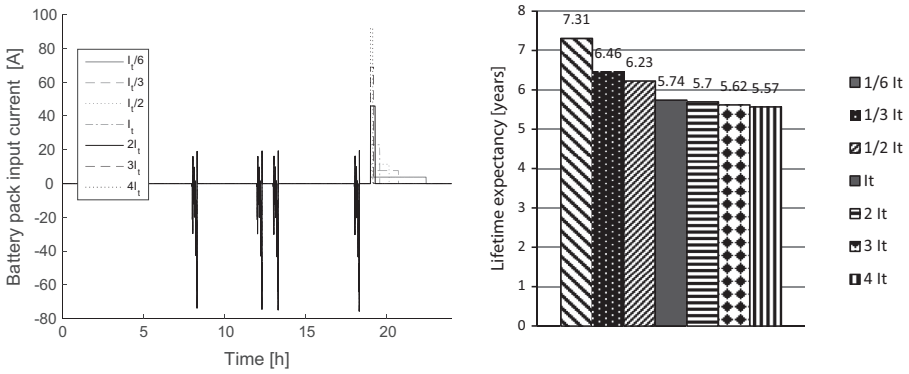

(a) Current profile during charging rates tests (b) Life time expectancy depending on charging rates

Fig. 7. Current profiles and results of the charging rates simulations.

the charge time is small enough to cause a negligible cycling aging compared to the calendar aging and the lifetime expectancy tends to a minimal value around 5.5 years.

4.2. Influence of V2G

4.2.1. Case studies

In addition to the daily duty cycle presented earlier, several charging and discharging phases are added. The discharging phase represents the vehicle connected to grid sections where the energy stored in the vehicle is used to relieve the grid during high demand periods. The constant charges and discharges are performed at a 40 A rate and stopped whenever the SOC reaches 10% or 90%. As a consequence 5 test cases scenarios have been defined (Fig. 8):

- The reference case consists in a classical daily use with a simple recharge when the driver comes back home.
- The "just in time" case consists in charging the car just before the first trip in the morning.
- During the "charge when you can" case the driver tries to charge the car whenever they have time to do so (that is after every trip except when they get back home for lunch).
- The "strong V2G" scenario consists in a discharge of the car when there is time (at 9 AM, 2 PM and 7 PM) and a recharge when the battery is empty before leaving (6 AM, 11 AM, 4 PM). As a consequence, the battery is mostly stored at a low SOC (10%).
- The "light V2G" scenario is only considering a discharge of the battery when the driver comes back home at the end of the day.

These test case scenarios deal with two main stress factors regarding aging, which are current inside the cells and the SOC. Another stress factor of aging to take into account is the temperature.

4.2.2. Results

The simulation evaluates the aging of the batteries during one year's use, considering that the profile patterns described in Fig. 8 occur every day. In Fig. 9 are represented the capacity losses for both technologies for every test case.

Due to the sizing differences between both packs, we will not focus on the comparison of the raw performances of both technologies but rather on the differences that can be seen between the test case behaviors.

For both cells, the best scenario is the "just in time" case. In this scenario, the cell remains at low SOC during the night, reducing the calendar aging effect compared to the reference case where it is stored at 90% SOC. It is even more visible in the "charge when you can" scenario for the LFP/C based battery where the cell is always stored at 100% SOC increasing capacity loss during storage. Yet the "strong V2G" scenario where the battery is always stored at 10% SOC is not so good compared with the reference case for both technologies. In this case the advantage from storage at low SOC is outweighed due to the need to recharge the battery to 100% SOC before every use. This recharge causes a higher cycle aging capacity loss and thus a premature aging.

However, the behavior seen in the case of a LFP/C based battery is different from the one encountered with a NCA/C based battery where the aging of the "charge when you can" scenario is slightly bigger than the reference case but stays in the same order of magnitude. Moreover it clearly appears that in the case of the NCA/C based pack, the V2G scenarios lead to a premature aging of the battery (4% loss for the strong V2G and 2.8% for light V2G) and are even worse than the "charge when you can" scenario (2.7% loss). However, for the LFP/C battery this last scenario is the worst one (7.6% loss) and the light V2G is the second best scenario with similar aging to the "just in time" case (around 3.5% loss). It seems that the NCA/C based battery studied here is more sensitive to cycle aging than calendar aging. Therefore it will perform worse when submitted to frequent charges (eg. during V2G and "charge when you can" scenarios). This same kind of result has been observed by Guenther et al. [22] where frequent charges have a negative impact on battery state of health.

This result can be verified by estimating the aging rate given by Eqs. (2) and (4) assuming for simplicity an initial capacity loss of 1 Ah, at 288 K and for both batteries a 1.7 I_t charging rate (as in our V2G simulations). It appears that the calendar aging rate of the A123s cell is twice that for the Saft cell at SOC between 30% and 65% whereas the cycling aging rate is only 25% higher. As a consequence it is clear that the overall aging will be lower for the Saft cell but the impact of cycling aging will be higher.

As a consequence, both technologies exhibit clearly different behaviors when submitted to the same test cases. Based on these simulations, advice for vehicle use and especially recommendations on V2G applications will be different depending on the technology used to build the battery pack.

5. Conclusion

A generic empirical capacity aging model for Li-ion batteries has been developed. It is coupled with an electrothermal model and accounts for both types of aging encountered during Li-ion battery life: calendar aging and cycle aging. In order to describe calendar

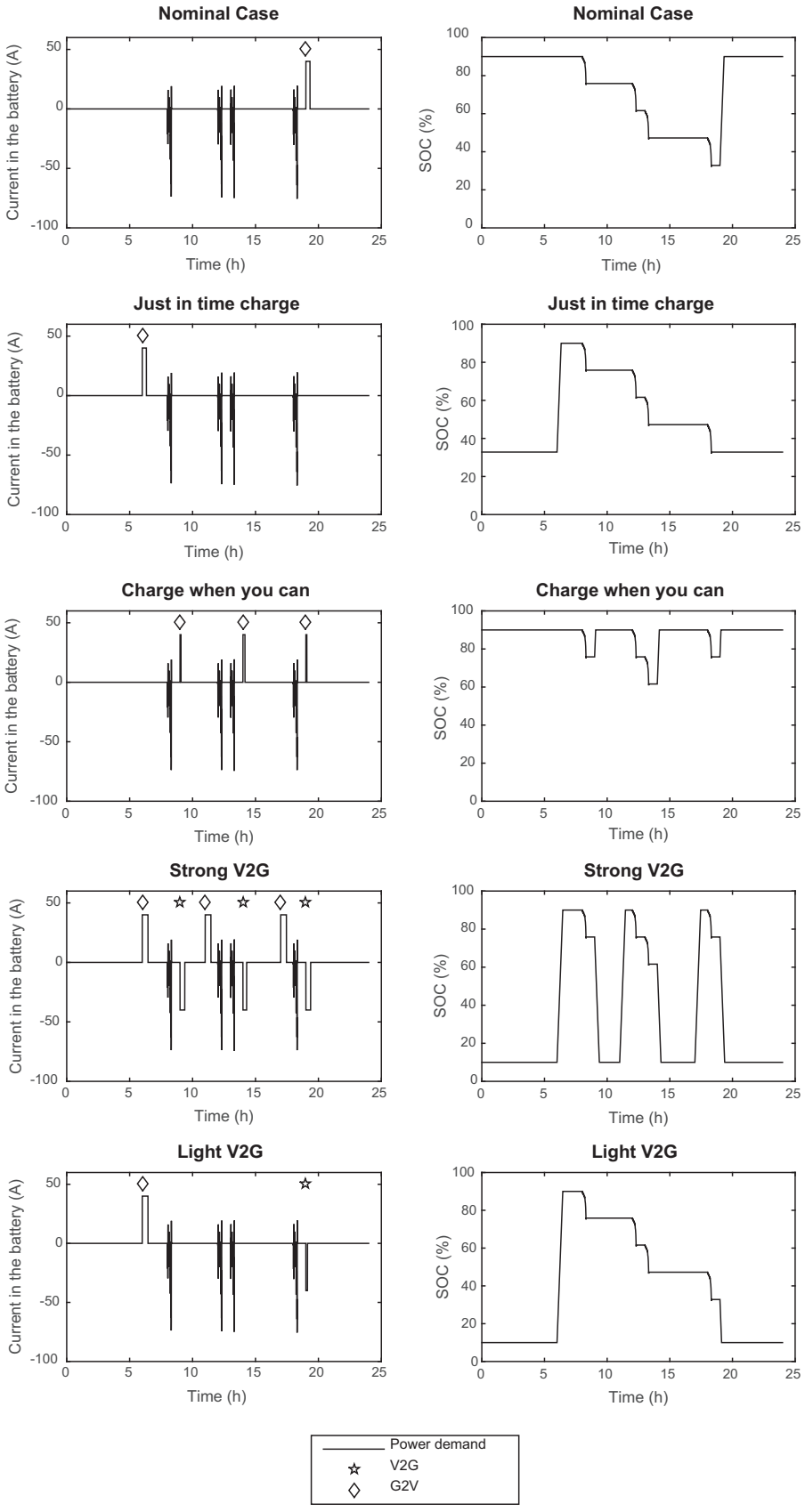

Fig. 8. Current and SOC profiles during test case scenarios.

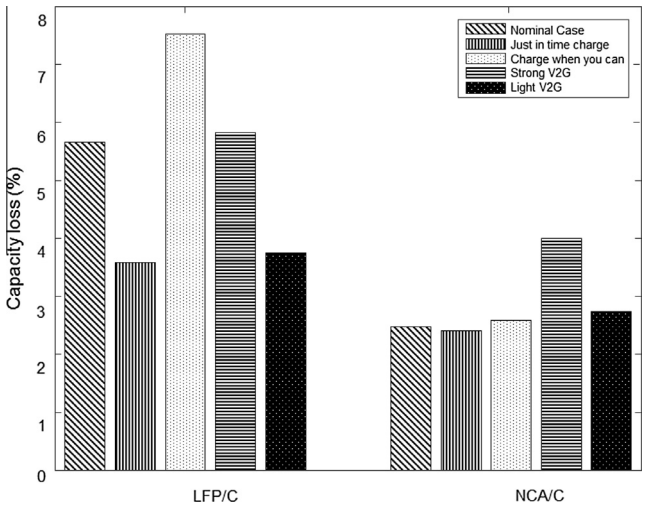

Fig. 9. Capacity loss for both battery technologies after 1 year cycle according to every scenario.

and cycling aging, only two stress factors were chosen: SOC and temperature for calendar aging and current and temperature for cycling. Thanks to an extensive experimental campaign and data mining, and despite the limited number of stress factors, it has been possible to calibrate and validate the model for two different Li-ion technologies on synthetic and realistic vehicle profiles. Once validated, the model has been integrated in a system simulation software application in order to assess the behavior of the cells when submitted to various test case scenarios. These simulations were able to show the influence of fast charging on the battery aging and showed some major differences between both technologies, the NCA/C based battery proved to be more sensitive to cycle aging compared to the LFP/C cell, leading to a premature aging when submitted to frequent charges in V2G scenarios.

This approach proved to be appropriate in order to evaluate the charging strategies that could be applied to an electrical vehicle in order to increase its battery lifetime and cost efficiency. It has been used to accurately model the specific behaviors of both cells used in this study, and this approach leads to the recommendation that a light V2G strategy should be used for the LFP/C based cell, while it should be avoided in the case of the NCA/C based battery. Thanks to our original modeling approach based on a differentiated capacity loss, it is possible to use this aging model on various applications without requiring any modification or recalibration. It is also worth noting that this approach has been successfully applied to two different Li-ion technologies.

This study only focuses on the capacity loss due to aging. However, it is known that batteries also exhibit resistance increase. This increase has been neglected here, since, in the case of both cells used, this resistance increase remains low even at the end of life, with a resistance increase around 10% for the A123s cell [15] and below 15% for the Saft cell. However, for other cells this may not be the case. As a consequence further work should be done in order to apply this approach for power loss.

References

[1] Vetter J, Novak P, Wagner MR, Veit C, Moller KC, Besenhard JO, et al. Ageing mechanisms in lithium-ion batteries. J Power Sources 2005;147(1–2):269–81.
[2] Nykvist B, Nilsson M. Rapidly falling costs of battery packs for electric vehicles. Nat Clim Change 2015;5(4):329–32.
[3] Broussely M, Biensan P, Bonhomme F, Blanchard P, Herreyre S, Nechev K, et al. Main aging mechanisms in Li ion batteries. J Power Sources 2005;146(1–2):90–6.
[4] Legrand N, Knosp B, Desprez P, Lapicque F, Raël S. Physical characterization of the charging process of a Li-ion battery and prediction of Li plating by electrochemical modeling. J Power Sources 2014;245:208–16.
[5] Zhang Q, Guo Q, White RE. Semi-empirical modeling of charge and discharge profiles for a $LiCoO_2$ electrode. J Power Sources 2007;165(1):427–35.
[6] Kassem M, Bernard J, Revel R, Pélissier S, Duclaud F, Delacourt C. Calendar aging of a graphite/$LiFePO_4$ cell. J Power Sources 2012;208(0):296–305.
[7] Kassem M, Delacourt C. Postmortem analysis of calendar-aged graphite/$LiFePO_4$ cells. J Power Sources 2013;235(0):159–71.
[8] Groot J, Swierczynski M, Stan AI, Kær SK. On the complex ageing characteristics of high-power $LiFePO_4$/graphite battery cells cycled with high charge and discharge currents. J Power Sources 2015;286:475–87.
[9] Klett M, Eriksson R, Groot J, Svens P, Högström KC, Lindström RW, et al. Non-uniform aging of cycled commercial $LiFePO_4$//graphite cylindrical cells revealed by post-mortem analysis. J Power Sources 2014;257:126–37.
[10] Spotnitz R. Simulation of capacity fade in lithium-ion batteries. J Power Sources 2003;113(1):72–80.
[11] Wang J, Liu P, Hicks-Garner J, Sherman E, Soukiazian S, Verbrugge M, et al. Cycle-life model for graphite-$LiFePO_4$ cells. J Power Sources 2011;196(8):3942–8.
[12] Ecker M, Nieto N, Käbitz S, Schmalstieg J, Blanke H, Warnecke A, et al. Calendar and cycle life study of $Li(NiMnCo)O_2$-based 18,650 lithium-ion batteries. J Power Sources 2014;248:839–51.
[13] Bloom I, Potter BG, Johnson CS, Gering KL, Christophersen JP. Effect of cathode composition on impedance rise in high-power lithium-ion cells: long-term aging results. J Power Sources 2006;155(2):415–9.
[14] Newman J, Thomas-Alyea KE. Electrochemical systems. 3rd ed. Hoboken, New Jersey: John Wiley & Sons, Inc; 2004.
[15] Prada E, Di Domenico D, Creff Y, Bernard J, Sauvant-Moynot V, Huet F. A simplified electrochemical and thermal aging model of $LiFePO_4$-graphite Li-ion batteries: power and capacity fade simulations. J Electrochem Soc 2013;160(4):A616–28.
[16] Safari M, Morcrette M, Teyssot A, Delacourt C. Multimodal physics-based aging model for life prediction of Li-ion batteries. J Electrochem Soc 2009;156(3):A145–53.
[17] Broussely M, Herreyre S, Biensan P, Kasztejna P, Nechev K, Staniewicz RJ. Aging mechanism in Li ion cells and calendar life predictions. J Power Sources 2001;97–98:13–21.
[18] Belt J, Utgikar V, Bloom I. Calendar and PHEV cycle life aging of high-energy, lithium-ion cells containing blended spinel and layered-oxide cathodes. J Power Sources 2011;196(23):10213–21.
[19] Ecker M, Gerschler JB, Vogel J, Käbitz S, Hust F, Dechent P, et al. Development of a lifetime prediction model for lithium-ion batteries based on extended accelerated aging test data. J Power Sources 2012;215:248–57.
[20] Schmalstieg J, Kabitz S, Ecker M, Sauer DU. From accelerated aging tests to a lifetime prediction model: analyzing lithium-ion batteries. In: IEEE, editor. 2013 world electric vehicle symposium and exhibition: 17–20 November 2013. Barcelona, Spain; 2013, p. 1–12.
[21] Sarasketa-Zabala E, Martinez-Laserna E, Berecibar M, Gandiaga I, Rodriguez-Martinez LM, Villarreal I. Realistic lifetime prediction approach for Li-ion batteries. Appl Energy 2016;162:839–52.
[22] Guenther C, Schott B, Hennings W, Waldowski P, Danzer MA. Model-based investigation of electric vehicle battery aging by means of vehicle-to-grid scenario simulations. J Power Sources 2013;239:604–10.
[23] Marongiu A, Roscher M, Sauer DU. Influence of the vehicle-to-grid strategy on the aging behavior of lithium battery electric vehicles. Appl Energy 2015;137:899–912.
[24] Bishop JD, Axon CJ, Bonilla D, Tran M, Banister D, McCulloch MD. Evaluating the impact of V2G services on the degradation of batteries in PHEV and EV. Appl Energy 2013;111:206–18.
[25] Bloom I, Cole BW, Sohn JJ, Jones SA, Polzin EG, Battaglia VS, et al. An accelerated calendar and cycle life study of Li-ion cells. J Power Sources 2001;101(2):238–47.
[26] Siemens Industry Software. LMS imagine. Lab Amesim: Electric Storage Library 13. User's Guide; 2014.
[27] Prada E, Bernard J, Mingant R, Sauvant-Moynot V. Li-ion thermal issues and modeling in nominal and extreme operating conditions for HEV/PHEV's. In: 2010 IEEE vehicle power and propulsion conference lille, France September 1–3, 2010. Piscataway, NJ; 2010.
[28] Prada E, Di Domenico D, Creff Y, Bernard J, Sauvant-Moynot V, Huet F. Simplified electrochemical and thermal model of $LiFePO_4$-graphite Li-ion batteries for fast charge applications. J Electrochem Soc 2012;159(9):A1508–19.
[29] Wright RB, Motloch CG, Belt JR, Christophersen JP, Ho CD, Richardson RA, et al. Calendar- and cycle-life studies of advanced technology development program generation 1 lithium-ion batteries. J Power Sources 2002;110(2):445–70.
[30] Jungst RG, Nagasubramanian G, Case HL, Liaw BY, Urbina A, Paez TL, et al. Accelerated calendar and pulse life analysis of lithium-ion cells. J Power Sources 2003;119–121:870–3.
[31] Grolleau S, Molina-Concha B, Delaille A, Revel R, Bernard J, Pelissier S, et al. The French SIMCAL research network for modelling of calendar aging for energy storage system in EVs and HEVs – EIS analysis on LFP/C cells. ECS Trans 2013;45(13):73–81.
[32] Gyan P, Aubret P, Hafsaoui J, Sellier F, Bourlot S, Zinola S, et al. Experimental assessment of battery cycle life within the SIMSTOCK research program. Oil Gas Sci Technol – Rev IFP Energies nouvelles 2013;68(1):137–47.

[33] Savoye F. Impact des impulsions périodiques de courant sur la performance et la durée de vie des accumulateurs lithium-ion et conséquences de leur mise en œuvre dans une application transport. PhD. Laboratoire Ampère; 2012.
[34] Bernard J, Revel R, Audigier D. How do life duty cycles govern the degradation mechanisms of LFP/C Li-ion batteries?: a case study. In: Batteries: the international energy & power supply conference and exhibition; 2013.
[35] Badin F, Le Berr F, Briki H, Dabadie J, Petit M, Magand S, et al. Evaluation of EVs energy consumption influencing factors, driving conditions, auxiliaries use, driver's aggressiveness. In: World electric vehicle symposium and exposition (EVS 27), 2013: Barcelona, Spain, 17–20 November 2013. Piscataway, NJ: IEEE; 2013. p. 1–12.